EXPLORE
Newsletter for the
Association of Applied Geochemists
www.appliedgeochemists.org
NUMBER 196 SEPTEMBER 2022

Standardization of field-portable short-wave infrared processing for mineral exploration

McLean Trott[1,2], Stephanie Sykora[4], Nicholas Jansen[5], Collette Pilsworth[1], Matthew Leybourne[1,3], Daniel Layton-Matthews[1]

[1]Department of Geological Sciences and Geological Engineering, Queen's University, 36 Union Street, Kingston, Ontario, Canada, K7L 3N6

[2]GoldSpot Discoveries Corp.,69 Yonge Street, Suite 1010, Toronto, Ontario, Canada, M5E 1K3

[3]Arthur B. McDonald Canadian Astroparticle Physics Research Institute, Department of Physics, Engineering Physics & Astronomy, Queen's University, Kingston, Ontario, Canada K7L 3N6

[4]OreQuest Consultants, 6891 Wiltshire St., Vancouver, BC, Canada, V6P 5H2

[5]Teck Resources Limited, Bentall 5, 550 Burrard St #3300, Vancouver, BC V6C 0B3

https://doi.org/10.70499/GQXJ2140

Introduction

Shortwave infrared (SWIR) spectroscopy began to enter the minerals industry as an exploration technique in the mid-1990s with the introduction of the Portable Infrared Mineral Analyzer (PIMA) by Integrated Spectronics (Thompson *et al.* 1999). Since that time, major advancements have occurred, including the continued development of spectral libraries for explorers to apply to various styles of ore deposits (Baldridge *et al.* 2009; Percival *et al.* 2016; Schodlok *et al.* 2016; Meerdink *et al.* 2019). Further research revealed that key spectral features related to mineral chemistry can be used by explorers to vector towards potential orebodies (Laakso *et al.* 2016; Neal *et al.* 2018; Cooke *et al.* 2020; Zhou *et al.* 2022). Within the last 10 years, spectral core scanning hardware has allowed large amounts of high-resolution spectral data to be acquired on drill cores (Tappert *et al.* 2011; Schodlok *et al.* 2016; Acosta *et al.* 2019; Tusa *et al.* 2019; Acosta *et al.* 2020).

The use of the SWIR technique using multi- and/or hyperspectral platforms has broad applications in mineral exploration, particularly for hydrothermal deposit types where alteration mineral zonation is well developed (Thompson *et al.* 1999; Hauff 2008). Commonly occurring alteration minerals that contain oxygen in water or hydroxyl bonds are SWIR-active and can be readily identified (Bishop *et al.* 2008), permitting the definition of alteration mineral patterns around potential orebodies (Duke 1994). In addition, subtle chemical variations of some minerals can be detected by changes in the wavelength position of key absorption features, which may be related to distance from a potential heat source and/or orebody (Neal *et al.* 2018; Cooke *et al.* 2020; Zhou *et al.* 2022). A third vector type involves calculating the crystallinity of minerals, such as white micas or kaolinite, which may indicate temperature of formation or degree of crystal development; likewise, crystallinity may also provide a proxy for distance to a potential hydrothermal source and/or orebody (Kübler 1968; Hauff *et al.* 1991; Scott and Yang 1997; Guggenheim *et al.* 2002; Wang *et al.* 2021). The three SWIR vector types described, alteration mineral patterns, mineral chemistry and crystallinity, are commonly difficult to identify visually (Crósta 1990). Deployment of SWIR platforms allow explorers to rapidly and inexpensively acquire data to detect these key vectors toward potential orebodies.

Currently, the mineral exploration industry is collecting large SWIR datasets, but in many cases without rigorous QA and QC (quality assurance and quality control) procedures in place. Suboptimal collection and processing practices may introduce problems with bulk processing (e.g., aiSIRIS™, The Spectral Geologist™ (TSG™)) and/or dataset fusion for subsequent interpretation and application of machine learning techniques. In addition, users who wish to interpret their SWIR datasets, but are not spectral experts, are commonly inundated with spectral outputs they do not know how to effectively apply, and for which the limitations may not be understood. This article provides guidance for effective data acquisition (with appropriate QA-QC measures in place), background for users to better interpret their SWIR spectral data, and examples of vectoring applications in the context of the calc-alkalic porphyry copper environment. A downloadable digital document associated with this article, "Field-portable SWIR acquisition, QA-QC, and processing guide" (herein referred to as the Guide), may be used to further explore this topic and construct a practical workflow. The intention is that new users start with an accessible framework, and that experienced practitioners consider some standardization procedures for their own workflows.

SWIR spectroscopy

The method detects a range of the electromagnetic spectrum from 1300 – 2500 nm, recently described as SWIR 1 (1300 – 1850 nm) and SWIR 2 (1850 – 2600 nm), differentiated by their vibrational modes (Laukamp *et al.* 2021). Hardware limitations restrict the upper detection limit to 2500 nm. Certain bonds, primarily those involving oxygen or

continued on page 5

Standardization of field-portable short-wave infrared processing… *continued from page 1*

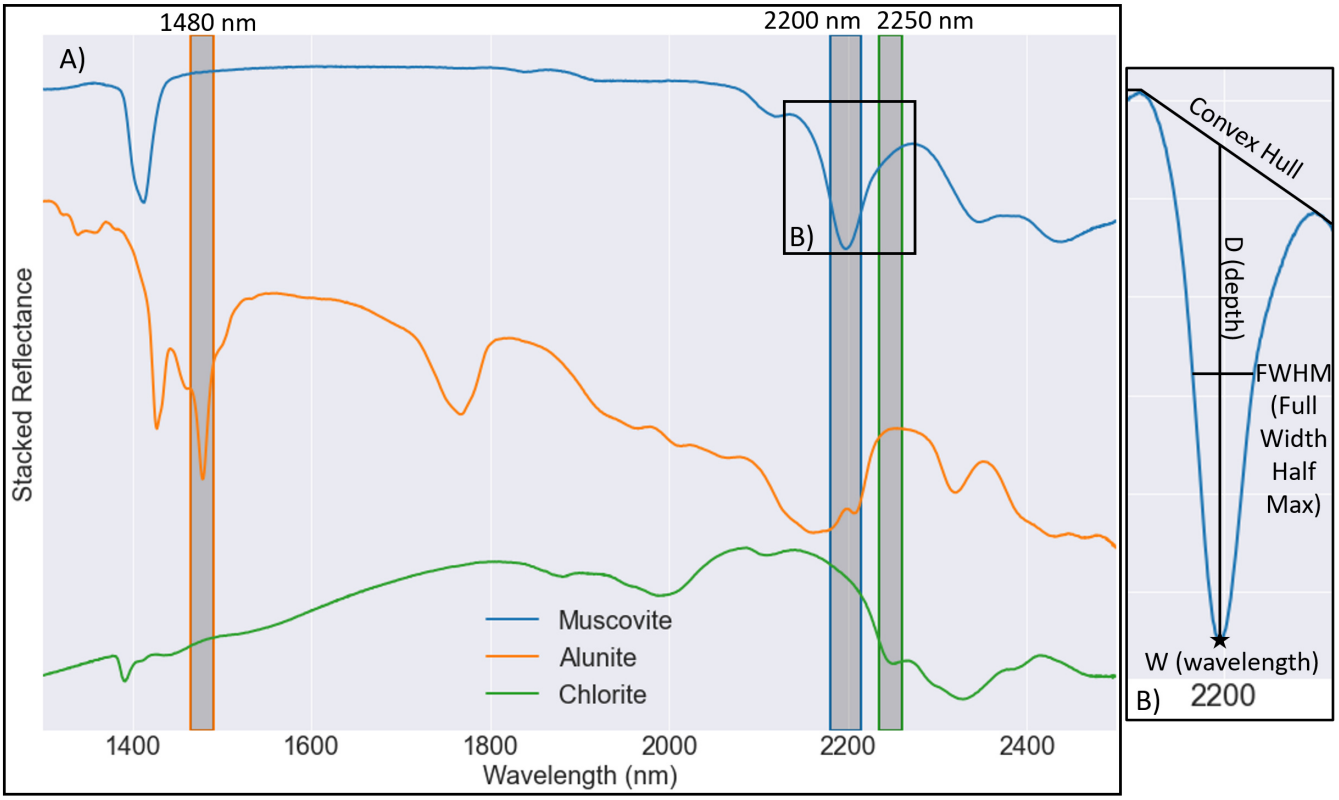

Figure 1. Examples of SWIR spectra extracted from the JPL Ecostress spectral library (Grove et al. 1992), showing key absorptions for the three minerals discussed as vectors. Inset (B) illustrates the nomenclature of absorption feature scalars applied to the 2200nm "AlOH" absorption for muscovite. Depth is measured from the base of the absorption (the minimum) vertically to where it intercepts the convex Hull line, formed by connecting apices along the spectral curve. FWHM is measured at the midpoint of D, between either side of the absorption feature.

ammonium, vibrate when impacted by energy at specific wavelengths within this range, converting some of the incident energy into kinetic energy and therefore reflecting a modified spectrum with lower intensity at the corresponding wavelength. In practical terms, this means shining a light on a sample, capturing the reflected spectra (Fig. 1), and processing the data such that the absorption features reveal the composition of the sample by comparing the geometry of absorption features (Fig. 1, inset B) to a specific SWIR-active mineral or combination of such minerals.

Scales of application

At regional scales, multispectral satellite systems (e.g., Landsat, ASTER, etc.) apply the same principles as field-portable (point data) hyperspectral techniques, although at a much coarser spectral and spatial resolution. In areas of abundant outcrop these satellite-borne methods may be useful for identifying the geometry of large alteration zonation patterns (Bedell *et al.* 2009). Due to limited spectral resolution, multispectral techniques can detect mineral groups, but it is commonly difficult to detect individual minerals; likewise, extracting mineral chemistry or crystallinity information can be challenging. At an intermediate scale, airborne hyperspectral systems can be used for greater spatial and spectral resolution than satellite systems; these airborne platforms can typically identify individual mineral species and extract some mineral chemistry information (Cudahy *et al.* 2001).

At the target scale, field-portable hyperspectral SWIR instruments (e.g., PIMA, Malvern Panalytical TerraSpec™, Spectral Evolution OreXplorer ™) have a high spectral and spatial resolution and can be used in a time- and cost-effective manner. In many cases, handheld methods and airborne or satellite systems are used in conjunction with each other, whereby handheld measurements can help contextualize results by constraining the spectral response of representative samples from an area of study (Lampinen *et al.* 2017).

In recent years, hyperspectral techniques have been applied using core scanning platforms (e.g., HyLogger®, CoreScan®, Terracore®, SisuROCK®), which collect abundant point readings or capture a spectrum per 'pixel' to produce a spectral image (at the ~500 µm to ~1.2 mm scale)(Cracknell *et al.* 2019; Barker *et al.* 2021). These instruments provide exponentially more information and are most effectively applied at the mine-site to better characterize the rock for metallurgical studies (Lypaczewski *et al.* 2019; Byrne *et al.* 2020).

continued on page 6

Standardization of field-portable short-wave infrared processing… *continued from page 5*

Field-portable SWIR

The scale of application discussed herein focuses on spectra collected with field-portable instrumentation. Instruments like these typically expose a sample to a light source through a window with an approximately 2 cm diameter, and then route the reflected light back to sensors and a processing unit to capture a spectrum. Spectra are ultimately downloaded from the unit and can be processed by cloud-based, largely automated software (e.g., IMDEX's aiSIRIS™) or by using other semi-automated spectral interpretation products like CSIRO's (the Commonwealth Scientific and Industrial Research Organization) The Spectral Geologist™ (TSG™) software (Berman *et al.* 1999). Generally, the output can potentially identify up to 5 mineral species in a spectrum and extract geometric information for relevant absorption features, such as the width (or full width half maximum, FWHM), depth (D), and wavelength at minimum (W), as shown in Figure 1 inset B.

QA-QC considerations

Consistent data collection with QA-QC controls is critical, especially for large projects with multiple users, over a long period, and potentially with multiple instruments. Wavelength differences of up to 5 nm for W1480 (alunite-related) and 2 nm for W2200 (white mica-related) for the same samples analyzed using distinct instruments have been documented (Chang and Yang 2012; Uribe-Mogollon and Maher 2020). Proper standardization allows for robust interpretation and facilitates application of machine learning techniques, which tend to require 'apples-to-apples' feature inputs. The need for guidelines and standards in this space has been highlighted previously (Kerr *et al.* 2011).

Ideally, the analysis should be conducted in an environment with consistent lighting, however, good contact between the instrument and rock surface should minimize noise related to fluctuations in variable lighting conditions (Trott *et al.* in preparation). Good contact is achieved by ensuring that the interface between the sample window and sample medium is such that no large gaps exist where ambient light might enter the instrument-sample interface. This is straightforward for flat surfaces or loose material but uneven (e.g., roughly fractured) or rounded (e.g., drill core) surfaces may merit the use of a rubber grommet between the instrument and surface, such as that found around the sample window of a contact probe. Rock chips (1 to 5 mm, e.g., RC chips) provide the best medium for sample representativity; fine pulps generate noisy spectra and should not be used. Spectra can be captured for residual soils, sieved to a standard size (e.g., -80 mesh), and may be particularly useful combined with traditional soil geochemistry data. A critical requirement is that the sample is dry, as H_2O is spectrally active. Samples can be dried in a sunny area or an oven at temperatures less than ~40 °C, as higher temperatures could change the structure of some clays (e.g., convert smectite to illite) (Russell and Farmer 1964).

The first mandatory QA-QC measure for SWIR spectrometers includes measuring a Spectralon™ white reference disc comprised of a fluoropolymer with nearly 100% reflectance in the SWIR range (Bruegge *et al.* 1993); if the various sensors in the instrument are functioning properly and the instrument is calibrated it will produce a flat line spectrum. The Spectralon™ disc can also act as a ´blank´ to determine if there is any dust or debris in the analytical probe. Most instruments are shipped with at least one Spectralon™ white reference disc. Care must be taken to keep them clean and not touch the upper surface, as skin oils can contaminate the spectral response. Contaminated discs can be recovered by wet sanding the surface with fine carbide sandpaper and allowing it to dry overnight.

A second mandatory QA-QC measure is the analysis of a Mylar® 'standard', which has five pronounced absorptions (1128.7, 1660.1, 1952.9, 2131.6, and 2256.0 nm) allowing the user to determine the accuracy of their instrument and whether it is within calibration limitations (i.e. within ± 1 nm of the known absorption feature wavelength). The ideal method for analyzing the Mylar® standard is by placing it on top of the Spectralon™ disc. Mylar® is readily available at most art supply stores. We also recommend usage of an in-house standard consisting of a mineral with a relatively homogeneous composition and that occurs in the study area; ideal candidates might be white mica (illite, paragonite, muscovite, phengite), kandite (halloysite, kaolinite, nacrite, dickite), alunite, and/or a chlorite-rich sample. The Mylar® and in-house standards allow

continued on page 8

Note: *This EXPLORE article has been extracted from the original EXPLORE Newsletter. Therefore, page numbers may not be continuous and any advertisement has been masked.*

Standardization of field-portable short-wave infrared processing… *continued from page 6*

the user to track accuracy and variation in key absorptions features (e.g., 2200 nm "Al-OH" feature, alunite absorption, etc.) over time and between instruments, allowing results to be leveled, if necessary. Analytical duplicates (duplication of an analysis spot) are also recommended to ascertain the precision of results. These QA-QC measures should be used at the beginning and end of the analysis session and periodically (intervals of ~ 20 measurements) throughout the session. Key metadata that should be recorded at the time of collection include reading ID, user, date, instrument model and serial number, analysis time, and sample medium (e.g., rock, drill core, rock chips, QA-QC sample type, etc.). Instructions for evaluating QA-QC results are provided in the Guide, as well as a TSG template for extracting Mylar scalars (Appendix B: Mylar_QAQC_scalars.tsg).

Processing

Historically users required specialization in a very manual process of identifying mineral species from individual spectra, a time-consuming endeavor with the quality of results highly dependent on the expertise of the user. A commercial solution to this, aiSIRIS™, consists of a cloud-based, largely automated software wherein uploaded spectra are classified relative to a large library of expert-interpreted spectra. For users who wish to interpret spectra in a more involved way, The Spectral Geologist™ (TSG™) software enables bulk processing of large volumes of spectra through i) its implementation of 'The Spectral Assistant' to unmix spectra against a pure mineral reference library for mineral identification and ii) extract 'scalars' to quantify the geometry (shape) of key absorption features (Berman *et al.* 1999; Huntington *et al.* 1999). TSG is appropriate for bulk processing tasks but still requires a certain level of prior knowledge to operate effectively and reduce the resulting data into useful vectors, a subject which is discussed at length in the *Guide*.

SWIR in mineral exploration: porphyry copper vectoring

Zonation patterns of alteration minerals with respect to hydrothermal deposit types are generally well established. These patterns may be observed upon visual inspection, but subtleties in alteration facies are commonly more difficult to differentiate, particularly in so-called "white rock" alteration zones such as the advanced argillic and phyllic (or "sericitic") zones of a porphyry copper system. In the case of the advanced argillic assemblage, the distribution of white, commonly fine-grained clay or sulfate minerals such as kaolinite, alunite, dickite, diaspore, pyrophyllite, zunyite, or topaz has distinct implications in terms of pH and temperature of formation and by proxy, relative distance to hydrothermal source and/or potential orebody. These minerals are commonly difficult to differentiate visually but are easily identified using SWIR methods. Figure 2 illustrates the broad geometric relationships between porphyry copper alteration assemblages and the physicochemical character of their SWIR-active mineral assemblages.

3D examination of SWIR mineral matches from systematically collected drill core data may prove vital in defining alteration assemblages and patterns, which provide indications towards mineralization, informing further drilling. These insights may prove crucial in an industry where exploration search spaces are becoming more complex, on peripheries of ore systems and under post-mineral cover.

The substitution chemistry of some mineral types may be examined through its spectral response (Bishop *et al.* 2008). Tschermak-type substitution, where Al is replaced by (Fe, Mg) + Si in white mica minerals (illite, phengite, paragonite, and muscovite) can be captured by examination of the wavelength at minimum (W2200) of the Al-OH absorption feature (Swayze *et al.* 1992; Duke 1994; Halley *et al.* 2015; Cloutier *et al.* 2021). This substitution is controlled by factors like pH and concentrations of Fe^{2+} and K^{+} in the hydrothermal fluid (Halley *et al.* 2015) as it reacts with country rock and precipitates white mica minerals during the formation of phyllic/sericitic alteration assemblages in a porphyry system. More specifically, the value of W2200 shifts from ~2190 to 2225 nm as white micas increasingly substitute (Fe, Mg) + Si for Al (Cloutier *et al.* 2021; Laukamp *et al.* 2021), transitioning from paragonitic to phengitic composition (Fig. 2).

Another potential SWIR vector involves estimation of the Mg# for chlorite-dominated spectra, observed in a wavelength shift of the "Fe/Mg-OH" absorption feature found around 2250 nm (W2250), and strongly coupled with a wavelength shift in the "Mg/Fe-OH" absorption feature (W2340) (Lypaczewski and Rivard 2018; Neal *et al.* 2018). Higher W2250 values indicate higher Fe relative to Mg, and vice versa (McLeod *et al.* 1987; Scott *et al.* 1998; Huntington *et al.* 1999; Jones *et al.* 2005; Bishop *et al.* 2008; Lampinen *et al.* 2017). The "Fe/Mg-OH" W2250 absorption feature is preferred over the "Mg/Fe-OH" W2350 because it occurs within a higher signal-to-noise region and has less overlap with other spectral-active minerals, unlike the W2350, which overlaps with carbonate minerals (Bishop *et al.* 2013). In settings containing alunite, the shift in the absorption feature around 1480 nm has been shown to be related to the K:Na ratio (Bishop and Murad 2005), where higher wavelengths indicate an increasing Na content corresponding to a higher temperature of formation, and by proxy, closer to the potential heat source and/or an underlying porphyry intrusion (Fig. 2; (Chang *et al.* 2011; Cooke *et al.* 2020)).

The crystallinity of white micas (illite, paragonite, muscovite, and phengite) can be estimated by division of the "Al-OH" feature depth (D2200) by the depth of the water absorption feature occurring at 1900 nm (D1900) (Doublier *et al.* 2010b; Medina *et al.* 2021). Under higher temperatures of formation, white micas tend to crystallize with a more ordered structure and as a result incorporate less water in interlayered smectites, proxied by the relative depths (spectral abundances) of

continued on page 10

Standardization of field-portable short-wave infrared processing… *continued from page 8*

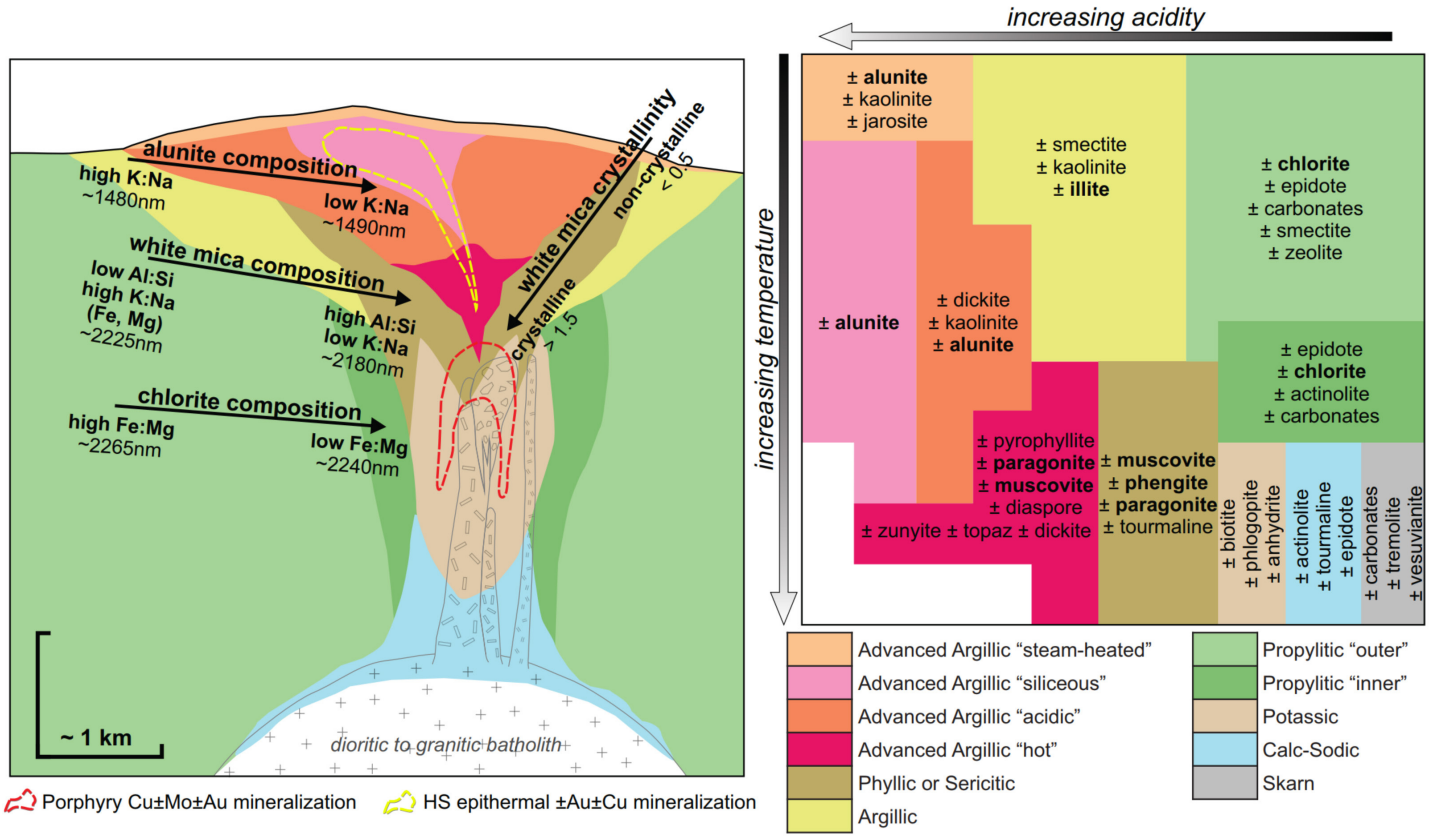

Figure 2. Idealized alteration pattern around a calc-alkalic Cu-Mo ± Au porphyry deposit (A-vein type). Discussed SWIR vectors shown on the left. Simplified acidity vs temperature diagram from (Corbett and Leach 1998) on the right with only key SWIR-identifiable minerals shown. Minerals in bold correspond to common SWIR vectors. Porphyry model modified from (Hedenquist et al. 2000; Seedorff et al. 2005; Sillitoe 2010; Halley et al. 2015; Hedenquist and Arribas 2022). Common porphyry SWIR-active alteration minerals, and properties of SWIR vectors, summarized from (Vedder and McDonald 1963; Kübler 1968; Hunt 1977; McLeod et al. 1987; Cathelineau 1988; De Caritat et al. 1993; Scott et al. 1998; Thompson et al. 1999; Bishop and Murad 2005; Bishop et al. 2008; Doublier et al. 2010a; Chang et al. 2011; Kamps et al. 2018; Neal et al. 2018; Cooke et al. 2020; Cloutier et al. 2021; Laukamp et al. 2021),
*Note that anhydrite is mentioned in the diagram. This cannot be detected directly by SWIR. Gypsum, however, is detectable and will be the output if anhydrite is present.

the "Al-OH" feature and 1900 nm water feature (Kübler 1967; Doublier *et al.* 2010b).

Method limitations

Critical to implementing SWIR effectively is an understanding of some basic method limitations. What follows is a non-exhaustive discussion of some of the more common limitations, and, where possible, mitigation steps.

Minerals without SWIR-active bonds are not detectable

Quartz (SiO_2), silica, or alteration assemblages characterized by pervasive silicification, do not contain SWIR-active bonds. Some providers identify quartz using an indirect/proxy method of detecting the H_2O feature produced by fluid

continued on page 11

Standardization of field-portable short-wave infrared processing… *continued from page 10*

inclusions hosted in quartz. This method should be approached with caution as the supposed quartz response can be confused by other spectral responses (e.g., wet core). Likewise, feldspars, sulfide minerals, spodumene, amongst many other minerals, cannot be detected with SWIR (Thompson *et al.* 1999).

Differences in spectral activity and albedo between minerals

Minerals with low spectral activity and/or albedo (overall reflectance) can be masked by those with high spectral activity and/or albedo. For example, minerals such as chlorite, biotite, or tourmaline have their most pronounced and diagnostic absorption features in the >2250 nm region where signal-to-noise is at its lowest, in contrast to other minerals, such as white micas and kandites, whose key absorption features occur in <2200 nm region where signal-to-noise is at its highest.

Compounding this problem are differences in albedo; where increased overall reflectance of lighter-colored minerals may make it difficult to identify less reflective minerals in the same analyzed material. In porphyry copper systems, for example, biotite in the potassic zone may not be detected if even a small amount of retrograde smectite or overprinting white mica is present. This is less problematic with high resolution core scanning techniques; smaller pixel sizes mean that the likelihood of obtaining pure spectra for a dark-colored mineral grain is higher.

A Non-quantitative method

Related to the previous two limitations, the quantification of mineral abundance in a sample is not possible; the inability to identify many major rock forming minerals such as quartz and feldspar, and the spectral over- or under-representation of certain minerals due to contrasting spectral activities and albedo. It is, however, possible to obtain an indication of “spectral abundance” or “spectral strength” calculated from absorption feature depths (D). These values are more likely to be related to spectral activity and albedo than modal abundance in the rock, although they may provide vectors of interest from the relative perspective.

White mica W2200 and the influence of kaolinite

The white mica W2200 mineral chemistry vectoring example described above is contingent on the spectra having been carefully filtered to remove any influence of kaolinite, a rather common mineral in both hypogene and supergene settings. Although variations in the W2200 value for white micas are indicative of mineral chemistry (Tschermak-type substitution), the W2200 value for kaolinite consistently occurs at approximately 2207 nm and, when present in a white mica sample, shifts the spectral response accordingly. A simple W2200 versus FWHM2200 plot can help filter out any influence of kaolinite, as shown in Figure 3. Vectoring using this feature requires carefully removing any white mica spectra that may have been influenced by the presence of kaolinite.

Host rock dependency for scalar values

Differences between hydrothermal fluid composition and wallrock reactivity (buffering characteristics) of the same deposit type but in distinct geological settings means that it is difficult to place universal ranges on scalar values. Relative changes on a case-by-case basis are useful for this reason, to examine pH/temperature gradients as opposed to seeking out any predefined or idealized value ranges. Additionally, the variability in scalar values lends itself to be more significant with a larger data set, where trends can be supported statistically.

Overprinted assemblages may not be visible

As with many other geoscientific methods, the most obvious signature is left by the final event in the evolution of a hydrothermal system. Overprinted assemblages tend to be retrograde altered or overwhelmed by minerals precipitated or recrystallized during later events, in some cases masking earlier events of greater economic significance (Cudahy *et al.* 2001; Jansen and Trott 2018; Trott *et al.* 2018).

continued on page 12

Standardization of field-portable short-wave infrared processing… *continued from page 11*

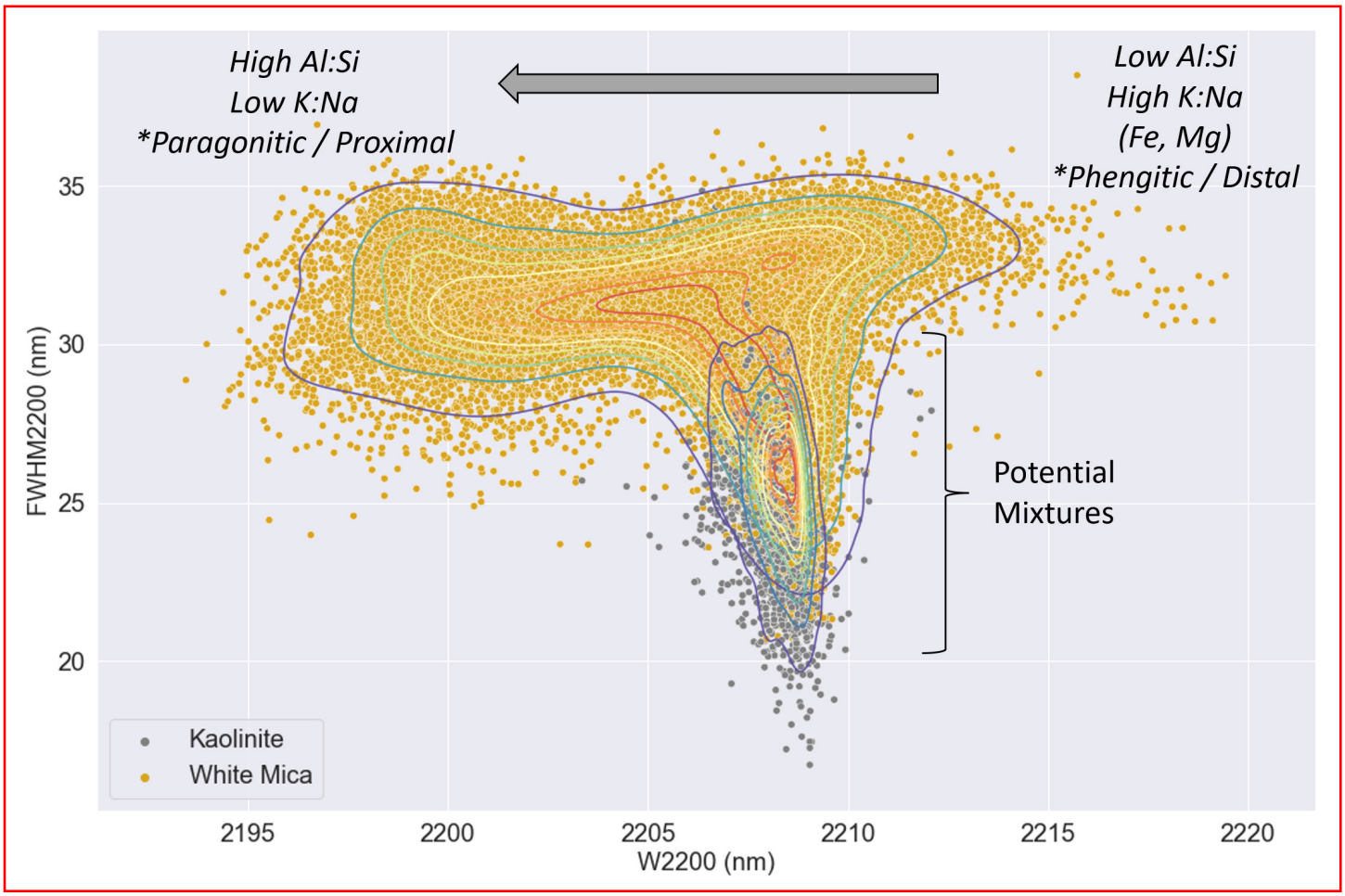

Figure 3. Spectra classified by TSG as white mica and kaolinite from a calc-alkalic porphyry (N=26506), with kernel density contours overlain for each species. Note the overlap between kaolinite and white mica spectra values in the subvertical density contours for kaolinite around 2208 nm; readings in this area must be used with caution when vectoring with W2200 due to likely influence of kaolinite on the white mica absorption position.

Field-portable SWIR-VNIR acquisition, QA-QC, and processing guide

The *Guide* and appendices can be accessed at https://www.appliedgeochemists.org/explore-newsletter/explore-issues. It begins with introductory material to introduce new users to the electromagnetic spectrum, progresses to discuss the SWIR range, followed by its application to mineral exploration. Sections 3, 4 and 5 are intended to be used as a guided walk-through to enable the reader to systematically reconstruct a workflow for capturing spectra with adequate QA-QC measures in place, process the results in TSG, and carry out post-processing operations necessary to derive valid vectors. Metadata capture, color scheme, and TSG template files are included as appendices.

Conclusions

With continued application of this method in the exploration industry; and access to standardization of acquisition and processing methodologies like those outlined here and detailed in the introduced processing manual, it is our hope that SWIR methods become more attractive as a low-cost exploration tool and, as data continues to be acquired, amenable to large-scale integration and interpretation, advanced data analytics and machine learning processes. As suggested here, adopting minimum standards for QAQC and processing routines are key to unlocking these potentials and increasing value to exploration processes from the SWIR method. We hope that the accompanying *Guide* facilitates the adoption of the method, and leading to ever-improving SWIR data quality, interpretation, and subsequent improved exploration outcomes.

Acknowledgements

We must thank the spectral geologists who paved the way for the invention, improvement, and uptake of this method in the geosciences: Anne Thompson and Phoebe Hauff for their tremendous contributions to the field; Scott Halley and Carsten Laukamp for directly and/or indirectly teaching and mentoring us (and many others) in this fascinating

continued on page 13

Standardization of field-portable short-wave infrared processing… *continued from page 12*

discipline; Sasha Pontual for bringing her knowledge to the world with her invention and popularization of aiSiris™ for bulk processing; and the talented group at CSIRO for their creation of TSG™, the tool that enabled us to explore what spectra mean and how best to apply the method in practice. Jon Huntington was extremely generous with his time and knowledge in editing this work. Finally, we thank Jeanne Percival and Bob Garrett for their comprehensive reviews, and Beth McClenaghan for encouraging us to complete this work and put it into the public domain for the benefit of others.

Supplementary material: "Field-Portable SWIR Acquisition, QA-QC, and Processing Guide, First Edition" ("the *Guide*") and related appendices are available at https://www.appliedgeochemists.org/explore-newsletter/explore-issues

References

Acosta, I.C.C., Khodadadzadeh, M., Tusa, L., Ghamisi, P. and Gloaguen, R. 2019. A machine learning framework for drill-core mineral mapping using hyperspectral and high-resolution mineralogical data fusion. *IEEE Journal of Selected Topics in Applied Earth Observations and Remote Sensing*, **12**, 4829-4842. https://doi.org/10.1109/jstars.2019.2924292.

Acosta, I.C.C., Khodadadzadeh, M., Tolosana-Delgado, R. and Gloaguen, R. 2020. Drill-core hyperspectral and geochemical data integration in a superpixel-based machine learning framework. *IEEE Journal of Selected Topics in Applied Earth Observations and Remote Sensing*, **13**, 4214-4228. https://doi.org/10.1109/jstars.2020.3011221.

Baldridge, A.M., Hook, S.J., Grove, C. and Rivera, G. 2009. The ASTER spectral library version 2.0. *Remote Sensing of Environment*, **113**, 711-715.

Barker, R.D., Barker, S.L.L., Cracknell, M.J., Stock, E.D. and Holmes, G. 2021. Quantitative mineral mapping of drill core surfaces II: Long-wave infrared mineral characterization using μXRF and machine learning. *Economic Geology*, **116**, 821-836, https://doi.org/10.5382/econgeo.4804.

Bedell, R., Crósta, A.P. and Grunsky, E. 2009. *Remote sensing and spectral geology*. Reviews in Economic Geology, Volume 16, Society of Economic Geologists (SEG).

Berman, M., Bischof, L. and Huntington, J. 1999. Algorithms and software for the automated identification of minerals using field spectra or hyperspectral imagery. *Proceedings of the 13th International Conference on Applied Geologic Remote Sensing*, 222-232.

Bishop, J.L. and Murad, E. 2005. The visible and infrared spectral properties of jarosite and alunite. *American Mineralogist*, **90**, 1100-1107.

Bishop, J., Lane, M., Dyar, M. and Brown, A. 2008. Reflectance and emission spectroscopy study of four groups of phyllosilicates: Smectites, kaolinite-serpentines, chlorites and micas. *Clay Minerals*, **43**, 35-54.

Bishop, J., Lane, M., Brown, A., Hiroi, T., Swayze, G. and Lin, J.-F. 2013. Spectral properties of Ca-, Mg-and Fe-bearing carbonates. *44th Annual Lunar and Planetary Science Conference*, 1719.

Bruegge, C.J., Stiegman, A.E., Rainen, R.A. and Springsteen, A.W. 1993. Use of Spectralon as a diffuse reflectance standard for in-flight calibration of earth-orbiting sensors. *Optical Engineering*, **32**, 805-814.

Byrne, K., Lesage, G., Gleeson, S.A., Piercey, S.J., Lypaczewski, P. and Kyser, K. 2020. Linking mineralogy to lithogeochemistry in the Highland Valley copper district: Implications for porphyry copper footprints. *Economic Geology*, **115**, 871-901, https://doi.org/10.5382/econgeo.4733.

Cathelineau, M. 1988. Cation site occupancy in chlorites and illites as a function of temperature. *Clay Minerals*, **23**, 471-485.

Chang, Z. and Yang, Z. 2012. Evaluation of inter-instrument variations among short wavelength infrared (SWIR) devices. *Economic Geology*, **107**, 1479-1488.

Chang, Z., Hedenquist, J.W. *et al.* 2011. Exploration Tools for Linked Porphyry and Epithermal Deposits: Example from the Mankayan Intrusion-Centered Cu-Au District, Luzon, Philippines*. *Economic Geology*, **106**, 1365-1398, https://doi.org/10.2113/econgeo.106.8.1365.

Cloutier, J., Piercey, S.J. and Huntington, J. 2021. Mineralogy, Mineral Chemistry and SWIR Spectral Reflectance of Chlorite and White Mica. *Minerals*, **11**, 471, https://doi.org/10.3390/min11050471.

Cooke, D.R., Agnew, P. *et al.* 2020. Recent advances in the application of mineral chemistry to exploration for porphyry copper–gold–molybdenum deposits: detecting the geochemical fingerprints and footprints of hypogene mineralization and alteration. *Geochemistry: Exploration, Environment, Analysis*, **20**, 176-188, https://doi.org/10.1144/geochem2019-039.

Corbett, G. and Leach, T. 1998. Southwest Pacific Rim Gold-Copper Systems: Structure, Alteration and Mineralization. *SEG Special Publication*, **6**.

Cracknell, M., Parbhakar-Fox, A., Jackson, L., Fox, N. and Savinova, E. 2019. Automated identification of sulphides from drill core imagery. *Proceedings of the 2019 Mineral Systems of the Pacific Rim Congress (PACRIM 2019)*, 79-82.

Crósta, A. 1990. Unveiling Mineralogical Information in Ore Deposits: the Use of Reflectance Spectroscopy for Mineral Exploration in South-America. Brazil. https://www.malvernpanalytical.com/en/learn/knowledge-center/application-notes/ANASDI20111110UnveilingMineralogicalInformationOreDeposits

continued on page 14

Standardization of field-portable short-wave infrared processing… *continued from page 13*

Cudahy, T.J., Wilson, J. *et al.* 2001. Mapping porphyry-skarn alteration at Yerington, Nevada, using airborne hyperspectral VNIR-SWIR-TIR imaging data. *IGARSS 2001. Scanning the Present and Resolving the Future. Proceedings. IEEE 2001 International Geoscience and Remote Sensing Symposium (Cat. No.01CH37217).* IEEE.

De Caritat, P., Hutcheon, I. and Walshe, J.L. 1993. Chlorite geothermometry: a review. *Clays and clay minerals*, **41**, 219-239.

Doublier, M., Roache, A. and Potel, S. 2010a. *Application of SWIR spectroscopy in very low-grade metamorphic environments: a comparison with XRD methods*. Geological Survey of Western Australia, Record 2010/7, 61 p.

Doublier, M.P., Roache, T. and Potel, S. 2010b. Short-wavelength infrared spectroscopy: A new petrological tool in low-grade to very low-grade pelites. *Geology*, **38**, 1031-1034, https://doi.org/10.1130/g31272.1.

Duke, E.F. 1994. Near infrared spectra of muscovite, Tschermak substitution, and metamorphic reaction progress: Implications for remote sensing. *Geology*, **22**, 621-624.

Grove, C., Hook, S.J. and Paylor III, E. 1992. *Laboratory reflectance spectra of 160 minerals, 0.4 to 2.5 micrometers.* Pasadena, CA: Jet Propulsion Laboratory.

Guggenheim, S., Bain, D.C. *et al.* 2002. Report of the Association Internationale pour l'Etude des Argiles (AIPEA) Nomenclature Committee for 2001: order, disorder and crystallinity in phyllosilicates and the use of the 'crystallinity index'. *Clay Minerals*, **37**, 389-393.

Halley, S., Dilles, J.H. and Tosdahl, R.M. 2015. Footprints: Hydrothermal Alteration and Geochemical Dispersion Around Porphyry Copper Deposits. *SEG Newsletter*, 1-7.

Hauff, P. 2008. An overview of VIS-NIR-SWIR field spectroscopy as applied to precious metals exploration. *Arvada, Colorado: Spectral International Inc*, **80001**, 303-403.

Hauff, P., Kruse, F., Madrid, R., Fraser, S., Huntington, J., Jones, M. and Watters, S. 1991. Illite crystallinity- Case histories using X-ray diffraction and reflectance spectroscopy to define ore host environments. *Thematic Conference on Geologic Remote Sensing, 8 th, Denver, CO*.

Hedenquist, J.W. and Arribas, A. 2022. Exploration implications of multiple formation environments of advanced argillic minerals. *Economic Geology*, **117**, 609-643.

Hedenquist, J.W., Arribas, A. and Gonzalez-Urien, E. 2000. Exploration for epithermal gold deposits, SEG REviews, 13, 245-277.

Hunt, G.R. 1977. Spectral signatures of particulate minerals in the visible and near infrared. *Geophysics*, **42**, 501-513.

Huntington, J., Cudahy, T. *et al.* 1999. Mineral mapping with field spectroscopy for exploration: Final report. *Commonwealth Scientific and Industrial Research Organization, Australia, Exploration and Mining Report*, **419**, 35.

Jansen, N. and Trott, M. 2018. NIR characteristics of porphyry copper deposits. Presented at the Resources for Future Generations (RFG), Vancouver, British Columbia, July 16-21, 2018.

Jones, S., Herrmann, W. and Gemmell, J.B. 2005. Short wavelength infrared spectral characteristics of the HW horizon: Implications for exploration in the Myra Falls volcanic-hosted massive sulfide camp, Vancouver Island, British Columbia, Canada. *Economic Geology*, **100**, 273-294.

Kamps, O.M., Van Ruitenbeek, F.J., Mason, P.R. and Van der Meer, F.D. 2018. Near-infrared spectroscopy of hydrothermal versus low-grade metamorphic chlorites. *Minerals*, **8**, 259.

Kerr, A., Rafuse, H., Sparkes, G., Hinchey, J. and Sandeman, H. 2011. Visible/infrared spectroscopy (VIRS) as a research tool in economic geology: background and pilot studies from Newfoundland and Labrador. *Geological Survey, Report*, **11**, 145-166.

Kübler, B. 1967. La cristallinité de l'illite et les zones tout à fait supérieures du métamorphisme. *Etages tectoniques*, 105-121.

Kübler, B. 1968. Evaluation quantitative du métamorphisme par la cristallinité de l'illite. *Bulletin Centre de Researches de Pau-SNPA*, **2**, 385-397.

Laakso, K., Peter, J., Rivard, B. and Gloaguen, R. 2016. Combined hyperspectral and lithogeochemical estimation of alteration intensities in a volcanogenic massive sulfide deposit hydrothermal system: A case study from Northern Canada. *2016 8th Workshop on Hyperspectral Image and Signal Processing: Evolution in Remote Sensing (WHISPERS).* IEEE, 1-5.

Lampinen, H.M., Laukamp, C., Occhipinti, S.A., Metelka, V. and Spinks, S.C. 2017. Delineating alteration footprints from field and ASTER SWIR spectra, geochemistry, and gamma-ray spectrometry above regolith-covered base metal deposits—An example from Abra, western Australia. *Economic Geology*, **112**, 1977-2003, https://doi.org/10.5382/econgeo.2017.4537.

Laukamp, C., Rodger, A. *et al.* 2021. Mineral physicochemistry underlying feature-based extraction of mineral abundance and composition from shortwave, mid and thermal infrared reflectance spectra. *Minerals*, **11**, 347, https://doi.org/10.3390/min11040347.

continued on page 15

Standardization of field-portable short-wave infrared processing… *continued from page 14*

Lypaczewski, P. and Rivard, B. 2018. Estimating the Mg# and AlVI content of biotite and chlorite from shortwave infrared reflectance spectroscopy: Predictive equations and recommendations for their use. *International journal of applied earth observation and geoinformation*, **68**, 116-126.

Lypaczewski, P., Rivard, B., Gaillard, N., Perrouty, S., Piette-Lauzière, N., Bérubé, C.L. and Linnen, R.L. 2019. Using hyperspectral imaging to vector towards mineralization at the Canadian Malartic gold deposit, Québec, Canada. *Ore Geology Reviews*, **111**, 102945.

McLeod, R., Gabell, A., Green, A. and Gardavsky, V. 1987. Chlorite infrared spectral data as proximity indicators of volcanogenic massive sulphide mineralisation. *Pacific Rim 87. International congress on the geology, structure, mineralisation and economics of Pacific Rim*, 321-324.

Medina, C.M., Ducart, D.F., Passos, J.S. and de Oliveira, L.R. 2021. Exploration vectoring from the white mica spectral footprint in the atypical auriferous Lavra Velha deposit, San Francisco Craton, Brazil. *Ore Geology Reviews*, **139**, 104438.

Meerdink, S.K., Hook, S.J., Roberts, D.A. and Abbott, E.A. 2019. The ECOSTRESS spectral library version 1.0. *Remote Sensing of Environment*, **230**, 111196.

Neal, L.C., Wilkinson, J.J., Mason, P.J. and Chang, Z. 2018. Spectral characteristics of propylitic alteration minerals as a vectoring tool for porphyry copper deposits. *Journal of Geochemical Exploration*, **184**, 179-198, https://doi.org/10.1016/j.gexplo.2017.10.019.

Percival, J., Olejarz, A. *et al.* 2016. The National Mineral Reference Collection (NMC) Digital Spectral (VIS-NIR-SWIR) Library. Part I: The Kodama clay mineral collection, Geological Survey of Canada, Open File 7923, 24 pp.

Russell, J.t. and Farmer, V. 1964. Infra-red spectroscopic study of the dehydration of montmorillonite and saponite. *Clay Minerals Bulletin*, **5**, 443-464.

Schodlok, M.C., Whitbourn, L. *et al.* 2016. HyLogger-3, a visible to shortwave and thermal infrared reflectance spectrometer system for drill core logging: functional description. *Australian Journal of Earth Sciences*, **63**, 929-940, https://doi.org/10.1080/08120099.2016.1231133.

Scott, K. and Yang, K. 1997. Spectral reflectance studies of white micas. *Australian Mineral Industries Research Association Ltd. Report*, **439**, 35.

Scott, K., Yang, K. and Huntington, J. 1998. The application of spectral reflectance studies of chlorites in mineral exploration. *North Ryde NSW: CSIRO Exploration & Mining Report*, **545**.

Seedorff, E., Dilles, J.H. *et al.* 2005. Porphyry deposits: Characteristics and origin of hypogene features.

Sillitoe, R.H. 2010. Porphyry copper systems. *Economic Geology*, **105**, 3-41.

Swayze, G., Clark, R.N., Kruse, F., Sutley, S. and Gallagher, A. 1992. Ground-truthing AVIRIS mineral mapping at Cuprite, Nevada. *JPL, Summaries of the Third Annual JPL Airborne Geoscience Workshop. Volume 1: AVIRIS Workshop*.

Tappert, M., Rivard, B., Giles, D., Tappert, R. and Mauger, A. 2011. Automated drill core logging using visible and near-infrared reflectance spectroscopy: A case study from the Olympic Dam IOCG deposit, South Australia. *Economic Geology*, **106**, 289-296, https://doi.org/10.2113/econgeo.106.2.289.

Thompson, A.J., Hauff, P.L. and Robitaille, A.J. 1999. Alteration mapping in exploration: application of short-wave infrared (SWIR) spectroscopy. *SEG Discovery*, 1-27.

Trott, M., Munchmeyer, C. and Valenzuela, C. 2018. The Valeriano porphyry copper deposit revisited: 3D geological/geochemical integration and characterization. *Resources for Future Generations 2018*, June 2018, Vancouver, Canada.

Trott, M., Pilsworth, C., Monte-Marcellino, B., Leybourne, M. and Layton-Matthews, D. in preparation. Time series evaluation of environmental variables and acquisition parameters on the quality of SWIR spectra. *TBD*.

Tusa, L., Andreani, L., Khodadadzadeh, M., Contreras, C., Ivascanu, P., Gloaguen, R. and Gutzmer, J. 2019. Mineral mapping and vein detection in hyperspectral drill-core scans: Application to porphyry-type mineralization. *Minerals*, **9**, 122.

Uribe-Mogollon, C. and Maher, K. 2020. White mica geochemistry: Discriminating between barren and mineralized porphyry systems. *Economic Geology*, **115**, 325-354.

Vedder, W. and McDonald, R. 1963. Vibrations of the OH ions in muscovite. *The Journal of Chemical Physics*, **38**, 1583-1590.

Wang, L., Percival, J.B., Hedenquist, J.W., Hattori, K. and Qin, K. 2021. Alteration mineralogy of the Zhengguang epithermal Au-Zn deposit, northeast China: Interpretation of shortwave infrared analyses during mineral exploration and assessment. *Economic Geology*, **116**, 389-406, https://doi.org/10.5382/econgeo.4792.

Zhou, Y., Wang, T. *et al.* 2022. Advances on exploration indicators of mineral VNIR-SWIR spectroscopy and chemistry: A review. *Minerals*, **12**, 958.